410 ka weak monsoon event recorded by stalagmites in Jinfo Cave of Chongqing

XU Yibin[1]，YANG Xunlin[1,2,3]，YUAN Daoxian[1,2,4]，HU Mingguang[1]，GE Xiaoyan[1]，GONG Meng[1]

（ 1. *School of Geographical Sciences, Southwest University/National Observation and Research Station of Karst Ecosystem in Jinfo Mountain of Chongqing*, *Chongqing* 400715, *China*；2. *Chongqing Key Laboratory of karst Environment*, *Chongqing* 400715, *China*；3. *Chongqing Nanchuan Field Base of Karst Ecological Environment*, *Ministry of Natural Resources*, *Chongqing* 400715, *China*；4. *Institute of Karst Geology*, *CAGS/Key Laboratory of Karst Dynamics*, *MNR & GZAR, Guilin, Guangxi* 541004, *China* ）

Abstract The freshwater discharge from melting ice sheets in the deglaciation or glaciation is prone to anomalies in ocean−atmosphere transport between different latitudes, which can lead to a series of abrupt millennial-scale climate events, either obvious or not, such as the Younger Dryas (YD) events and YD-like events. Marine Isotope Stage 11c (MIS 11c) serves as one of the best references for the current Holocene, and the studies of possible YD-like events and their triggering mechanisms during Holocene are conducive to the understanding of the occurrence pattern of extreme climate events. In this paper, the results of the study on the J33 δ^{18}O sequence records of stalagmites in Jinfo Cave, Chongqing, are shown: (1) Stalagmites in the Asian monsoon climate zone reveal a millennial-scale weak monsoon event that occurred around 410 ka BP prior to the Glacial Maximum of MIS 11 interglacial period. (2) Both the 410 ka weak monsoon event and the YD event occurred during the gradual strengthening of the monsoon and ascending branch of summer insolation in the Northern Hemisphere prior to the Glacial Maximum of interglacial period. This was also a time when Atlantic Meridional Overturning Circulation (AMOC) disturbance occurred. The duration, internal structure, and pattern of the events were similar, with differences in the change magnitude and ice volume conditions. (3) The weak monsoon event that occurred in 410 ka BP was primarily influenced by the combined effects of insolation and AMOC. This event was characterized by a sustained warming process that accelerated the melting of the Greenland ice sheet, leading to the destabilization of this ice sheet. The continuous flowing of freshwater into the North Atlantic resulted in a short-lived AMOC oscillation. The weakening of the AMOC resulted in a cold anomaly over the North Atlantic. As a result of atmospheric telecorrelation, the weaker AMOC led to a weaker Asian Summer Monsoon (ASM)

Key words Asian Summer Monsoon, MIS 11c, stalagmite δ^{18}O, weak monsoon event, Jinfo Cave, Southwest China

0　Introduction

The term "deglaciation" refers to the period from the Glacial Maximum when glaciers began to melt and retreat until they disappeared. Both in deglaciation and glaciation, freshwater discharge from melting ice bodies can cause anomalies in ocean−atmosphere transport between different latitudes, leading to a range of abrupt millennial-scale climate events, such as Younger Dryas (YD) events and YD-like events. Schulz et al[1] early dis-

covery of spontaneous and regular oscillations in the large-scale ocean circulation provided a theoretical foundation for the possibility of a YD-like event occurring in the mid to late Pleistocene. Sima et al[2] simulations indicated that YD-like events had occurred at the endpoint of every glaciation for the past 800 ka. Therefore, the YD events are not accidental at the end of the last deglaciation. The occurrence of YD-like events may be an intrinsic feature of glacial−interglacial cycle at the Middle and Late Pleistocene. Chen et al[3] discovered a

第 43 卷　第 2 期

XU Yibin, YANG Xunlin, YUAN Daoxian, et al: 410 ka weak monsoon event recorded by stalagmites in Jinfo Cave of Chongqing

229

YD-like event in the Asian monsoon region during the antepenultimate deglaciation. This event was likely a result of the coupled action of the Quaternary ice sheet and the large-scale ocean−atmosphere circulation. Similarly, Cheng et al.[4] identified a weak monsoon event during Termination III (T-III) that was similar to the YD event. Duan et al.[5] used stalagmite data from Kulishu cave in Northern China to demonstrate the existence of a weak monsoon event with a structure similar to the YD event during T-III. Because Marine Isotope Stage 11 (MIS 11)[6] has a higher degree of similarity in Earth orbital parameters than the Holocene[7], MIS 11 can serve as the most appropriate and direct palaeoclimate reference period for analogies to the Holocene and future climates[7]. At MIS 11, was there an event of millennial-scale climate change such as a YD-like event? The investigation of this issue can enhance our understanding of the driving mechanism behind the YD event and the dynamics of the glacial−interglacial transition[8]. The in-

vestigation can also provide a reference and basis for future climate predictions under similar boundary conditions. In this study, the oxygen isotope sequence of stalagmite J33 from Jinfo Cave, Chongqing was established, with the use of U-Th dating and stable isotope measurements. The aim is to investigate whether YD-like events occurred in the Asian monsoon climate zone during MIS 11.

1　Study Area, Materials and Methods

Samples of stalagmite J33 were collected from Jinfo Cave, located in Nanchuan district, Chongqing Municipality. Jinfo Mountain (29°01′N, 107°11′E) is situated in the junction zone between the southeastern edge of the Sichuan basin and the northern edge of the Yunnan−Guizhou Plateau (Fig.1). Influenced by both the Indian and East Asian monsoons, the study area falls under a typical subtropical humid monsoon climate
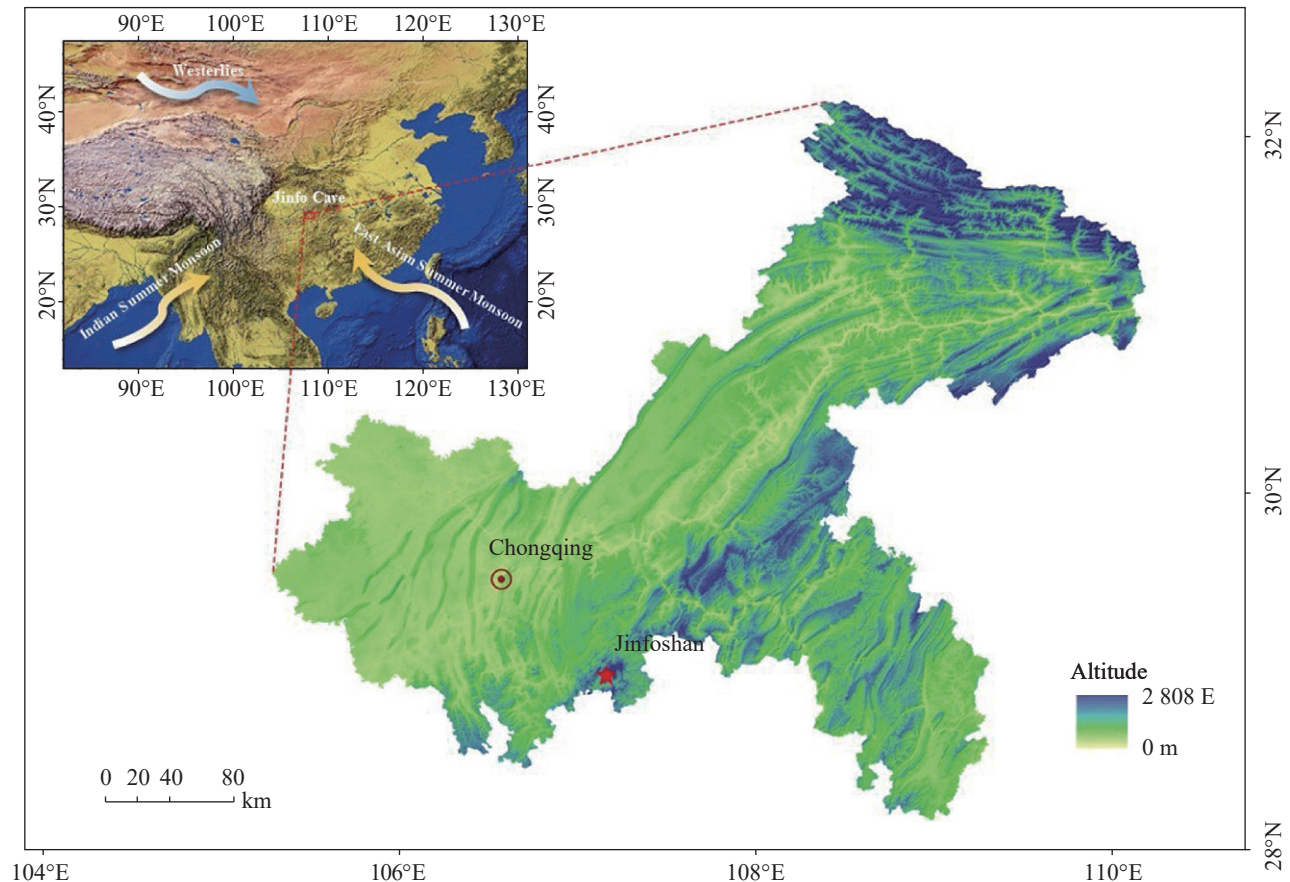

Fig. 1　Location of Jinfo Cave

which is mild with abundant rainfall, and is often cloudy and foggy. This area experiences an average annual relative humidity of over 90% and a long-term average temperature of 14.5 ℃. This area receives an average annual precipitation of 1,434.5 mm, unevenly distributed throughout the seasons. Precipitation from April to October accounts for more than 80% of the annual total[9]. The warm and rainy climate, with synchronous rain and heat, provides a favorable external environment for the development of vegetation, soil, and karst in the area[10].

Stalagmite J33 in Jinfo Cave measures 397 mm in length and 50 mm in diameter. It is cylindrical and grayish-black in color, and consists of densely crystallized calcite, dissected along its growth axis. In this study, the age samples and stable isotope samples of stalagmite J33 were analyzed. [230]Th age samples of stalagmite J33 were tested at the High Precision Mass Spectrometry and Environmental Change Laboratory (HISPEC) of National Taiwan University and the Isotope Laboratory of the Department of Geology and Geophysics of the University of Minnesota, U.S.A. Tests were conducted with the use of a multi-receiver plasma mass spectrometer (MC-ICP-MS) of Nepture Plus model. The dating method was based on the study of Cheng et al[11], with an age error of ≤1% (2σ).

The oxygen and carbon isotope samples of the stalagmite were analyzed at the Geochemistry and Isotope Laboratory of Southwest University and the Iso-

tope Laboratory of Nanjing Normal University with the use of Delta-V-Plus mass spectrometry-linked carbonate autosampling device (Kiel IV) and Finnigan MAT-253 mass spectrometer equipped with Kiel III. The collected samples, each with a quantity of 50−100 μg, were placed in the reaction vials in the tray. To ensure accuracy, one laboratory standard sample was inserted for every nine collected samples. The stability of the instrument was checked with the use of the international standard sample NBS19. Then, online testing was carried out once the instrument status was stabilized. The $\delta^{18}O$ values were obtained based on Vienna Pee Dee Belemnite (VPDB) standard, with an analytical error of ±0.06 ‰ (±1 σ).

2 Results

In this study, eight new age samples of stalagmite J33 were tested. The age data were arranged in the order of stalagmite deposition, indicating the data credibility[12] (Table 1). The age data of stalagmite J33 demonstrated an average age error of 1.8 ka, ranging from a maximum of 3.2 ka to a minimum of 1.3 ka. The age model of stalagmite J33 in Jinfo Cave (Fig.2) was constructed through linear interpolation. The stalagmite was deposited continuously with an average growth rate of about 5.9 mm·ka^{-1}. From 425.2 to 409.4 ka BP, the average growth rate of the stalagmite was 6.5 mm·ka^{-1}. During 409.4 to 393.5 ka BP, its average growth rate was 5.4

Table 1   [230]Th date results for stalagmite J33 ('*' indicates the new measured data.)

Sample Number	Depth (mm)	^{238}U (ppb)	^{232}Th (ppt)	$^{230}Th / ^{232}Th$ (atomic×10^{-6})	$\delta^{234}U$ (measured)	$^{230}Th / ^{238}U$ (activity)	Age (ka BP) (uncorrected)	Age (ka BP) (corrected)	$\delta^{234}U_{Initial}$ (corrected)
J33-1	144.9	2 516.4±0.1	884.9±10.2	72 003.1±832.5	424.5±0.3	1.536±0.001	393.5±2.0	393.5±2.0	1 288.5±7.5
J33-2	185.7	2 875.4±0.1	429.4±10.7	167 329.4±4 184.0	406.4±0.3	1.516±0.001	400.6±1.5	400.6±1.5	1 258.9±5.3
J33-3	196.9	2 158.7±0.1	2 182.9±11.0	24 635.3±127.0	402.8±0.3	1.511±0.002	400.9±3.2	400.9±3.2	1 248.6±11.2
J33-4	230.9	3 113.8±0.2	1 397.6±9.8	55 814.2±391.3	406.0±0.3	1.519±0.001	409.4±1.6	409.4±1.6	1 288.8±5.9
J33-5	268.7	2 791.5±0.2	738.7±28.7	95 730.9±3 715.6	416.4±0.3	1.536±0.001	415.6±1.6	415.6±1.6	1 345.7±6.1
J33-6	301.2	2 906.0±0.1	479.0±8.4	154 689.1±2 718.8	422.2±0.3	1.546±0.001	420.5±1.8	420.5±1.8	1 383.2±7.1
J33-7*	306.0	3 621.9±8.7	672.0±1.6	137 821.0±39.0	425.2±0.3	1.551±0.000	421.1±1.3	421.1±1.3	1 395.4±5.3
J33-8*	333.0	3 173.3±7.7	607.6±1.5	134 437.0±38.0	431.6±0.4	1.561±0.000	425.2±1.5	425.2±1.5	1 432.7±6.2

U decay constants: $\lambda_{238} = 1.551\,25×10^{-10}$[13] and $\lambda_{234} = 2.822\,06×10^{-6}$[9]. Th decay constant: $\lambda_{230} = 9.170\,5×10^{-6}$[11]. $\delta^{234}U = ([^{234}U/^{238}U]_{activity} - 1) ×1000$. $\delta^{234}U_{initial}$ was calculated based on ^{230}Th age (T), i.e., $\delta^{234}U_{initial} = \delta^{234}U_{measured}×e^{\lambda_{234}×T}$. Corrected ^{230}Th ages assume the initial ^{230}Th/^{232}Th atomic ratio of 4.4±2.2×10^{-6}. Those are the values for a material at secular equilibrium, with the bulk earth ^{232}Th/^{238}U value of 3.8. The errors are arbitrarily assumed to be 50%. "BP" stands for "Before Present" where the "Present" is defined as the year 1950 CE.

a.

393.5±2.0 ka BP

400.6±1.5 ka BP
400.9±3.2 ka BP

409.4±1.6 ka BP

415.6±1.6 ka BP

420.5±1.8 ka BP
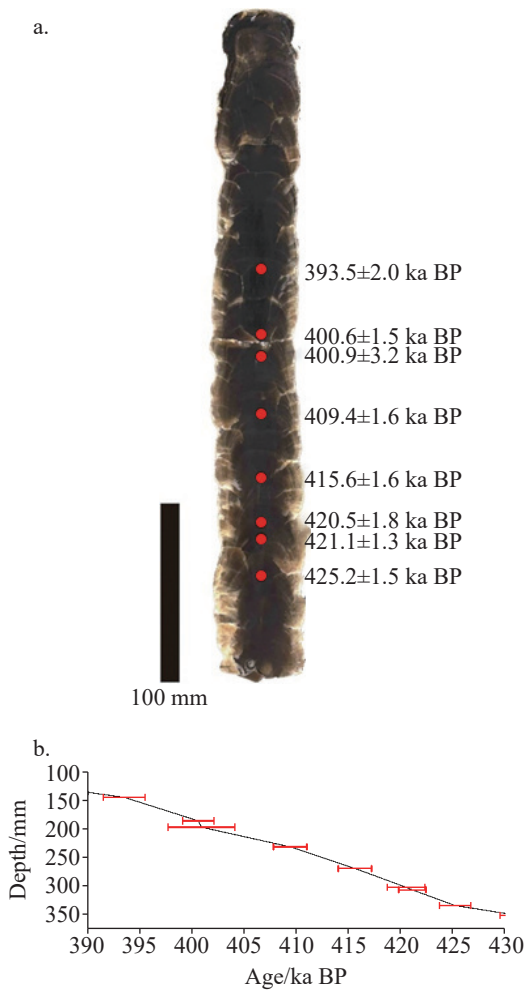421.1±1.3 ka BP

425.2±1.5 ka BP

100 mm

b.

Fig. 2　Profile of the stalagmite J33 (A) and age model (B)

The ages of stalagmite J33 were obtained by linear interpolation, and the red error bars in the figure indicate ^{230}Th ages and 2 σ errors.

$mm \cdot ka^{-1}$, which is slower.

In this study, the $\delta^{18}O$ records of stalagmite J33 from Jinfo Cave were compared with those of stalagmite SB14 from Sanbao cave. Both of the caves are situated in the Asian monsoon zone and are developed in the same time period[14]. Comparative results reveal similar overall trends (Fig.3) in that the records of these two stalagmites are significantly correlated (r=0.675, p< 0.01), passing the criterion of the reproducibility test[15].

Cheng et al.[16] noted that stalagmite $\delta^{18}O$ values in the region of East Asian Summer Monsoon (EASM) can generally indicate changes in summer monsoon intensity under ordinary climate conditions. That is to say, a positive $\delta^{18}O$ value will indicate a weakening of the summer monsoon, and vice versa. The comparability of
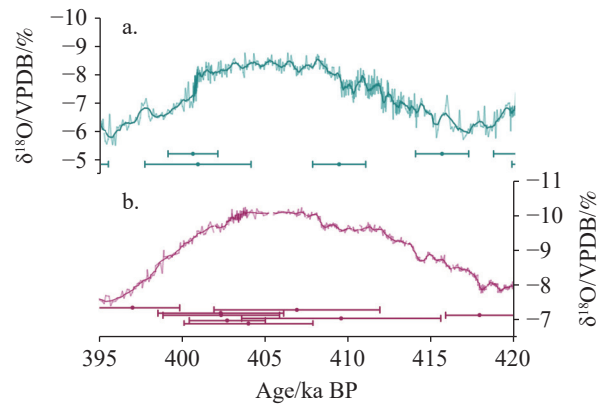

Fig. 3　Comparison of $\delta^{18}O$ values of stalagmite J33 in Jinfo Cave and of stalagmite SB14 in Sanbao cave

(A) $\delta^{18}O$ record of stalagmite J33 and dating errors (in this study); (B) $\delta^{18}O$ record of stalagmite SB14 and dating errors[13]

stalagmite $\delta^{18}O$ values with oceanic and ice core records on different time scales[17] has been supported by modeling studies[18]. The stalagmite $\delta^{18}O$ records from Hulu cave and Qingtian cave exhibit consistent changes on centennial or even shorter time scales based on annual stratigraphic time scales. Additionally, the consistent changes in $\delta^{18}O$ record and thickness of striation layer provide further support for the interpretation that stalagmite $\delta^{18}O$ records in East Asia can reflect changes in the intensity of the EASM[19]. Accordingly, the $\delta^{18}O$ values of stalagmite J33, located in the East Asian monsoon region, have been used as indicators of changes in EASM intensity.

3　Discussions

3.1　410 ka weak monsoon event

The $\delta^{18}O$ record of stalagmite J33 in Jinfo Cave (Fig.4), located in the East Asian monsoon region, reveals the weakening of monsoon on a millennial scale during the interglaciation of MIS 11 around 410 ka BP (hereafter referred to as the 410 ka weak monsoon event). The event lasted for about 1.1 ka (410.5− 409.4 ka BP), with a variability of about 1.1 ‰ (−8.1 ‰−−7.0 ‰). The EASM strengthened continuously at the beginning of MIS 11c (426−396 ka BP), which interrupted the strengthening of the monsoon and
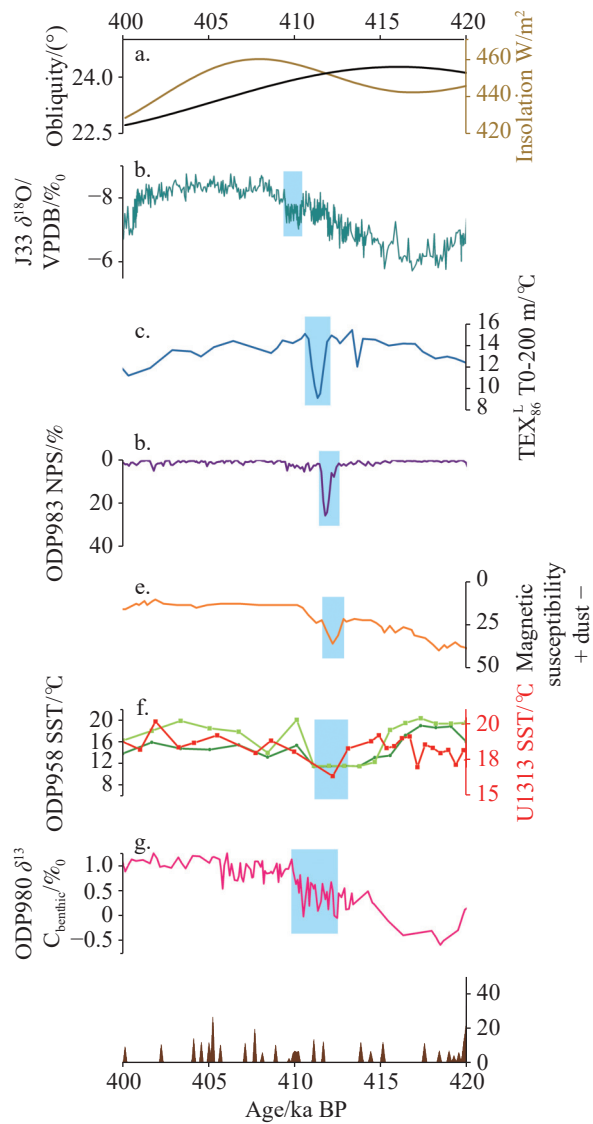
Fig. 4   410 ka BP weak monsoon event

(A) records of insolation (brown) and inclination (black) at 65 °N on July 21[22]; (B) δ18O record of stalagmite J33 and dating error (in this study); (C) δ18O record of stalagmite SB14 and dating error[14]; (D) record of temperature reconstruction for North Atlantic borehole M23414 0−200 m TEXL 86[23]; (E) record of North Atlantic borehole ODP983% N. pachyderma(s)[24]; (F) Magnetization rate-based record of wind-sand concentration in the central Red Sea[21]; (G) records of Alkenone- and foraminifera-based sea surface temperature (green and light green) from North Atlantic borehole ODP958[25] and records of alkenone-based sea surface temperature (red) from the Mid-Atlantic IODP U1313[26]; (H) ODP980 benthic foraminiferal δ13C record[27]; (I) ODP983 IRD record[22]. Blue bars in the figure indicate weak monsoon events or cold events.

delayed the onset of the Glacial Maximum of interglaciation in which the monsoon was strong and stable.

Atmospheric telecorrelation can transmit climate signals of anomalous cold or drought from the North Atlantic to intra-Asia[20]. Cheng et al[16] also noted a significant correlation between δ18O records of caves in China and North Hemisphere Summer Insolation (NHSI) and North Atlantic climate. Thus, our comparison with other paleoclimate records from around the world found that the weak monsoon event in 410 ka BP occurred during the rising phase of summer insolation at the high value of the inclination of Earth axis in the Northern Hemisphere (Fig.4A). Additionally, the record of temperature reconstruction for seawater TEXL 86 at 0−200 m from the North Atlantic borehole M23414 showed that the temperature of North Atlantic decreased significantly by 6 ℃ around 410 ka BP (Fig.4). The record of ODP983%N. pachyderma(s) also indicated a cooling event in the North Atlantic around 412 ka BP (Fig.4). Rohling et al[21] discovered a significant decrease in magnetization-based wind-dust concentrations in the central Red Sea in 412 ka BP (Fig.4). The record of ODP958 Sea Surface Temperature (SST) indicated a persistent bottom in North Atlantic SST in 413−411 ka BP, with a cooling range of 7−9 ℃ (Fig.4). Stein et al.[26] conducted a detailed analysis of the SST record from IODP Site U1313. They found that the SST record peaked at approximately 19 ℃ during MIS 11.3 (397−418 ka). However, this peak was interrupted by a brief cooling event around 413 ka BP (Fig.4). Prokopenko et al[28] identified a cooling event in the records of Pollen-spore BDP-99 in Lake Baikal of Russia. This event occurring about 411−410 ka BP was marked by an increase of the area covered by Pinus pumila and Pinus sibirica, which suggested a cooling of the Northern Hemisphere at high latitudes during that time period. In a study of high-resolution records from Site U1385 on the southwestern edge of the Iberian Peninsula, Oliveira et al[29] observed a significant decline in Mediterranean forest in ~411.6 ka BP, which could correspond to the short-term cooling observed in the record of Pollen MD01-2 443 at the same place[30]. However, the lower deposition rate at Site U1385 during the early MIS 11c prevented further discussion of this characteristic millennial-scale event. Around 410 ka BP, the climate deteriorated rapidly, affecting the Asian monsoon system at low, middle and high latitudes of the Northern Hemisphere.

XU Yibin, YANG Xunlin, YUAN Daoxian, et al: 410 ka weak monsoon event recorded by stalagmites in Jinfo Cave of Chongqing

第 43 卷　第 2 期

233

This also proved a global impact of this event.

The weak monsoon event was attributed to a combination of insolation and the Atlantic Meridional Overturning Circulation (AMOC). The weak monsoon event occurred during the early interglacial period of MIS 11 at a phase of rising NHSI and high values of inclination rate of Earth axis. A sustained strong warming process accelerated the melting, leading to the destabilization of the Greenland ice sheet. The continuous flowing of freshwater into the North Atlantic resulted in a short-lived AMOC oscillation[23]. Strong ocean heat transport helped to maintain interglacial conditions of low ice volume[31]. The weakening of the AMOC resulted in a cold anomaly over the North Atlantic. This anomaly caused temperature changes in this region and drove the movement of the Intertropical Convergence Zone (ITCZ)[32]. As a result of atmospheric telecorrelation, the weaker AMOC led to a weaker Asian Summer Monsoon (ASM)[17] i.e. the $\delta^{18}O$ anomalies recorded in stalagmite J33 of this study. John et al[33] demonstrated that around 410 ka BP, the Nordic oceans underwent extensive freshwater inflow at the onset of the climatic optimum. However, because the amplitude of precession was modulated by a smaller eccentricity, both the changes in precession and in insolation were small[7]. The limited melting of ice volume and freshwater discharge were due to the weaker NHSI. The North Atlantic Borehole ODP983 IRD did not record a significant IRD peak (Fig.4). Therefore, the weakening of the AMOC associated with this weak monsoon event was not sufficient to stop the AMOC and close the deep-water transport channel. The record of Site ODP980 in Fig.4 shows negative $\delta^{13}C$ in bottom water before the 410 ka weak monsoon event. This may indicate a weakening of North Atlantic Deep Water (NADW)[34] and a change in the flux pattern of North Atlantic Deep Water (NADW)[35], which in turn may lead to a perturbation of AMOC. Previous studies demonstrated that the instability and perturbation of AMOC during the early MIS 11c[36] resulted in a sudden weakening of the system, leading to the decrease of heat transport to the north and

the decrease of temperatures in the northern high latitudes. The cooling was then transmitted to the Asian monsoon region through the ocean−atmosphere system, ultimately resulting in a weakening of the ASM[37]. This explanation is supported by a simulation study conducted by Galaasen et al[35]. In their study on North Atlantic convective activity during the last few Glacial Maximums of interglacial period, they found that the AMOC could be perturbed even at the maximum of the interglacial period. The reduction of NADW could occur even if there were no large terrestrial ice sheets and no inflow of a large amount of freshwater. Oliveira et al[29] proposed that regulating cooling events on a millennial scale may involve positive feedback mechanisms on the AMOC related to freshwater from melting icebergs, variations in regional precipitation, and different impacts of iceberg discharge on deep water circulation and regional climate. Due to the absence of high-resolution paleoclimate records, the cause of the event remains a topic of debate.

3.2 Comparison with the YD event

In order to explore the similarity between the 410 ka weak monsoon event in the early part of MIS 11c and the YD event at the end of the last deglaciation, this study compares the features of the two events in detail (Fig.5), and finds that they share the following characteristics: (1) the same background of insolation at the time of the events. Both of these two weak monsoon events occurred during the gradual enhancement of NHSI before the Glacial Maximum of the interglacial period. (2) the same change patterns of the events. In the NGRIP $\delta^{18}O$ record from the Greenland ice core and the higher-resolution stalagmite record from Dongge cave, the YD events showed a "slow onset and fast end" pattern. The weak monsoon event during MIS 11c also showed the same transition. This event was preceded by a strong monsoon phase recorded in the J33 $\delta^{18}O$ sequence that corresponded to the Bølling-Allerød (BA) event. (3) the same internal structure of the events. Several studies have confirmed the high degree of climatic instability during the YD event[8]. The secondary cyclon-
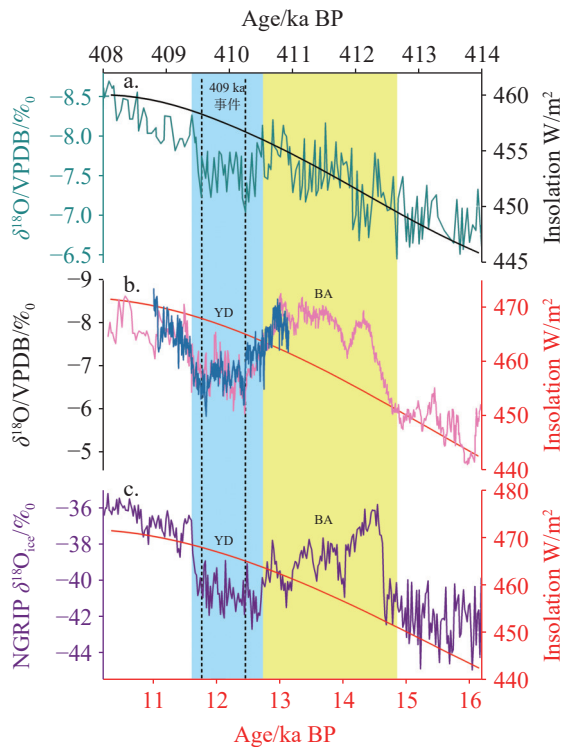
Fig. 5   Comparison between the 410 ka weak monsoon event and
the YD event (Adapted from Zhang Riping[38])

(A) Stalagmite J33 $\delta^{18}O$ record (green, in this study) and insolation record at
65 °N on July 21[22] (black); (B) record of stalagmite H82 $\delta^{18}O$ in Hulu
cave[39-40] (pink), record of stalagmite D4 $\delta^{18}O$[41] in Dongge cave (blue) and in-
solation record at 65 °N on July 21[22] (red); (C) NGRIP $\delta^{18}O$ record at AICC
2012 dating scale[42] (green) and insolation record at 65 °N on July 21[18] (red).
(A) is shown by the time coordinate of upper horizontal axis, and (B) and (C)
are shown by the time coordinate of lower horizontal axis. The blue bars in
the figure indicate weak monsoon events; the yellow bars indicate strong
monsoon events; and the black dotted lines respectively indicate the ending
time of the beginning phase and the starting time of the ending phase of the event.

ic variability on a centennial scale accounted for 2/3 of
the overall amplitude of the YD event[43]. The Atlantic
marine sedimentary record in mid- to low-latitudes
showed a series of rapid oscillations in tropical climate
on decadal scales[44-46]. Fig.5 displays frequent fluctu-
ations during the YD events in the NGRIP $\delta^{18}O$ record
and the stalagmite record in Dongge cave. At least 3−4
oscillations on decadal-to-centennial scales within the
weak monsoon event in stalagmite J33 $\delta^{18}O$ were recor-
ded. The internal structures of these two weak monsoon
events are very similar, both showing strong instability
and similar climate change characteristics of the weak-
ening of EASM[42-46]. (4) Both events experienced
AMOC perturbations. The YD event caused a signific-
ant weakening of the AMOC at high latitudes, as shown

in Fig.6, which had a greater impact on the ASM[47]. In
contrast, during the 410 ka weak monsoon event, the
negative trend in ODP980 $\delta^{13}C$ (Fig.6) reflected the
weakening of the NADW[34] and the change in the deep
Atlantic flux pattern[35], leading to an AMOC perturba-
tion that was not as pronounced or strong as that during
the YD event.

However, there are also some differences between
the 410 ka weak monsoon event and the YD event
shown in the records: (1) The durations were slightly
different. The duration of the 410 ka weak monsoon
event recorded by stalagmite J33 $\delta^{18}O$ was about 1.1 ka
(410.5−409.4 ka BP), and the duration of the YD event
recorded by stalagmite in Dongge cave was about 1.5 ka
(12.9−11.4 ka BP). It is evident that the YD event was
longer with more impact. (2) There was a difference in
the changing magnitude (Fig.6). The magnitude of the
410 ka weak monsoon event recorded by stalagmite J33
$\delta^{18}O$ was about 1.1‰, and the magnitude of the YD
event recorded by stalagmite in Dongge cave was
about 1.9‰. The magnitude of the former is signific-
antly smaller than that of the latter, and their intensit-
ies were also different. (3) The responses of different
types of greenhouse gas were different. As a sensitive
indicator of temperature change on a millennial scale,
the CH_4 record in Fig. 6 shows that a significant de-
crease occurred during the YD period, whereas the CH_4
concentration during the 410 ka weak monsoon event
experienced a decreasing trend but was not significant.
For CO_2, another type of greenhouse gas in Fig.6, the
concentration of CO_2 was higher and lasted for a longer
period during the 410 ka weak monsoon event than dur-
ing the YD period, but showed a brief downward trend,
which seemed to have some mitigating effect on the
melting of the ice sheet. In contrast to the relatively
stable CO_2 concentration during the YD period, the sig-
nificant change in CO_2 concentration during the 410 ka
weak monsoon event reflected the strong climate in-
stability during the event. Additionally, the warming
caused by the higher CO_2 concentration buffered the
cooling caused by the lower insolation at mid- to high-
latitudes in the Northern Hemisphere[51], resulting in
warming of the SST (Fig.4). (4) The ice volume condi-

第 43 卷　第 2 期

XU Yibin, YANG Xunlin, YUAN Daoxian, et al: 410 ka weak monsoon event recorded by stalagmites in Jinfo Cave of Chongqing
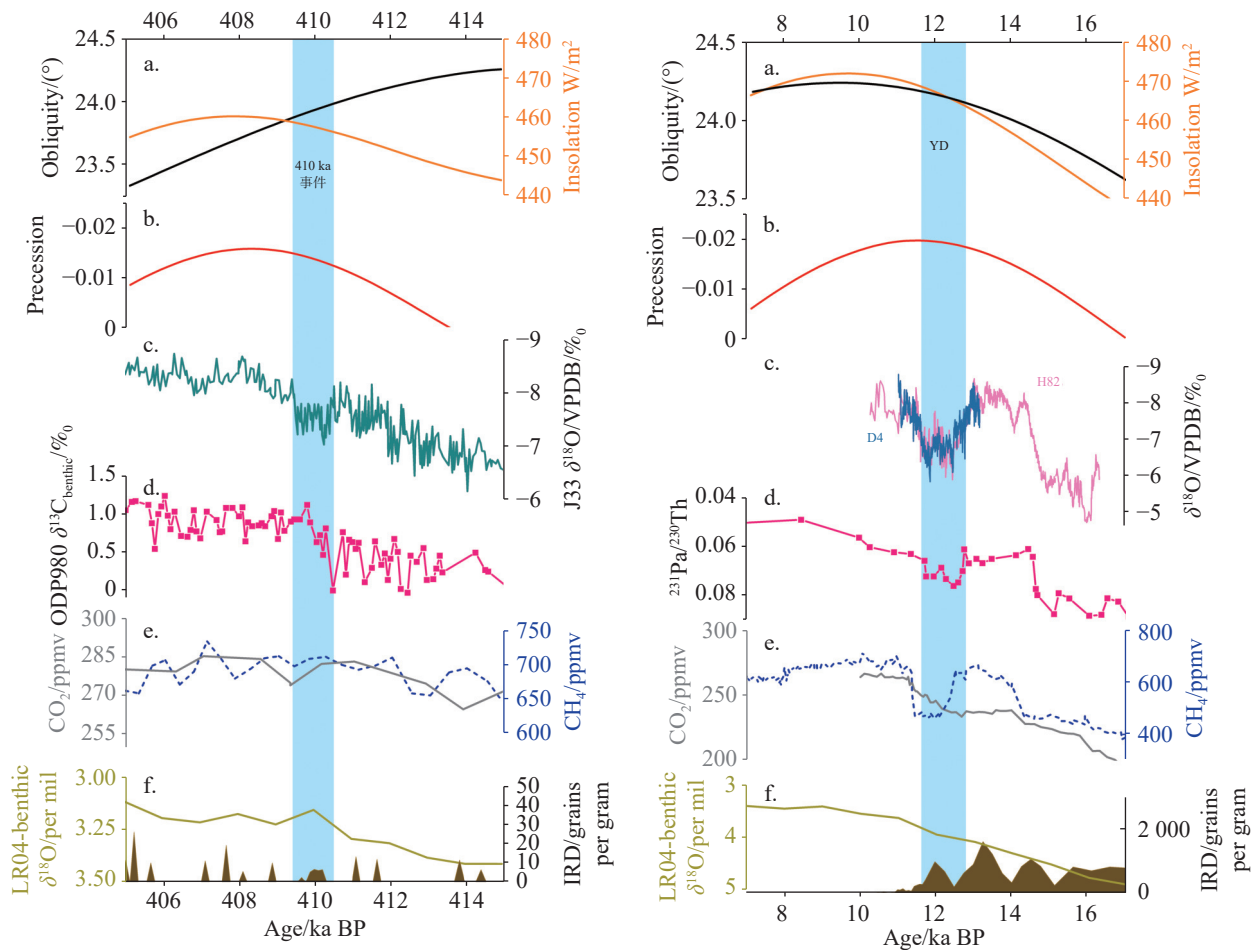
235

Fig. 6　Comparison of selected global records during the 410 ka weak monsoon event and the YD event

(A) records of insolation (brown) and inclination rate (black) at 65 °N on July 21[22]; (B) precession records[22]; (C) record of stalagmite J33 δ18O (turquoise on the left, in this study); δ18O record of stalagmite H82 in Hulu cave[39-40] (pink on the right,), δ18O record of stalagmite D4 in Dongge cave[41] (dark blue); (D) δ13C record of ODP980 benthic foraminiferal[26] (on the left); 231Pa/230Th ratio of marine sediments[48] (on the right); (E) records of Antarctic ice cores EDC CO2 (gray) and CH4 (blue)[49]; (F) LR04 δ18O record[50] and ODP983 IRD record[24]. The blue bars in Figure six indicate weak monsoon events or cold events.

tions are different (Fig.6). There is currently no literature supporting significant discharge of ice-drift debris during the 410 ka weak monsoon event. In contrast, strong discharge of ice-drift debris occurred during the YD event[52], which could explain why the latter was stronger than the former. Fig.6 illustrates that the δ18O recorded by LR04 gradually became negative during the YD event, indicating a decrease in ice volume and an increase in ice-drift debris. In contrast, during the 410 ka weak monsoon event, the δ18O fluctuated negatively with a very small amplitude, only 1/5 of the YD event, which indicated a small change in ice volume. This supports the viewpoint presented by Cheng et al[47] that the limited ice volume plays a minor role in driving the change of the low-latitude monsoon. (5) There are dif-

ferences in the Earth's orbital background. The YD event occurred in the range between the bottom of precession and the peak of inclination rate (Fig.6); therefore, the strong influence of precession and the high inclination rate contributed to the high level of NHSI values. This, in turn, accelerated the melting of the North Atlantic ice sheet and the discharge of freshwater[53]. In contrast, during the MIS 11 period, the amplitude of the YD event was moderated by smaller eccentricity, resulting in smaller variations in insolation[7]. During the 410 ka weak monsoon event, the solar inclination was significantly smaller than that during the YD event (Fig.6). This smaller inclination led to a reduction in high-latitude annual mean insolation[54], which is a favorable astronomical condition for triggering a sudden weakening of the

AMOC. Under the conditions of the 410 ka weak monsoon event occurring during a period of weak NHSI (Fig.6), the strong ocean heat transport helped to maintain the interglacial period with low ice volume[28]. This also suggests that there was no significant freshwater discharge during the weak monsoon event.

Both the 410 ka weak monsoon event and the YD event occurred during the gradual strengthening of the monsoon prior to the Glacial Maximum of the interglacial period. The ASM gradually strengthened with the increase of NHSI. However, the weak monsoon event interrupted the strengthening of monsoon. Additionally, the transition characteristics of the initial and final phases of the two weak monsoon events are remarkably similar. Both exhibited a change pattern of "slow onset and fast end" and were accompanied by AMOC perturbations, frequent internal oscillations on a short-time-scale, and similar internal characteristics. These findings suggest that the MIS 11 interglacial period played a crucial role in the development of the ASM, indicating that the climate variability event of MIS 11 on a millennial scale in the interglacial period is comparable to the YD event, and hence further supporting the comparability of MIS 11 with the Holocene. However, there are differences in the duration and amplitude of these two events. The different ice volume conditions at the time of the events led to significant differences in the behavior of the ice-drift debris. These differences are largely related to the NHSI and may be caused by the age error between different records.

4 Conclusions

(1) Before the Glacial Maximum of MIS 11 interglacial period, the J33 δ^{18}O sequence record of stalagmites in the Asian monsoon climate region shows a weak monsoon event that lasted for a millennium around 410 ka BP. Some paleoclimate records from the Northern Hemisphere also indicate this abrupt climatic change. However, higher-resolution climate records from the lower latitudes and the Southern Hemisphere are currently lacking to support this event.

(2) The 410 ka weak monsoon event and the YD event at the end of the last deglaciation is highly similar. Both events occurred during the ascending branch of NHSI and during the gradual strengthening of the monsoon before the Glacial Maximum of the interglacial period. In terms of internal structures, both events exhibit a change pattern of "slow onset and fast end", with frequent short-term oscillations and AMOC perturbations. However, there are differences in change amplitude and ice volume conditions that require further research.

(3) The 410 ka weak monsoon event was primarily caused by a combination of insolation and the AMOC. The sustained warming process accelerated the melting of the Greenland ice sheet, leading to its destabilization, while a continuous inflow of freshwater into the North Atlantic resulted in a short-lived oscillation of the AMOC. The weakening of the AMOC caused a decrease of temperature in the North Atlantic region, which in turn led to a weaker ASM through atmospheric telecorrelation.

Reference

［1］　Schulz M, Paul A, Timmermann A. Relaxation oscillators in concert: A framework for climate change at millennial timescales during the late Pleistocene［J］. Geophysical Research Letters, 2002, 29(24): 2193-2197.

［2］　Sima A, Paul A, Schulz M. The Younger Dryas-an intrinsic feature of late pleistocene climate change at millennial timescales［J］. Earth and Planetary Science Letters, 2004, 222(3-4): 741-750.

［3］　陈仕涛, 汪永进, 孔兴功, 刘殿兵, Edwards L R. 倒数第三次冰消期亚洲季风气候可能的类 Younger Dryas 事件［J］. 中国科学 D 辑: 地球科学, 2006(5)：445-452.

［4］　Cheng H, Edwards R L, Broecker W S, Denton G H, Kong X G, Wang Y J, Zhang R, Wang X F. Ice age terminations［J］. Science, 2009, 326(5950): 248-252.

［5］　Duan W H, Cheng H, Tan M, Ma Z B, Chen S T, Wang L S, Wang X F, Cui L L. Structural similarity between Termination III and I［J］. Quaternary Science Reviews, 2022(296): 0277-3791.

［6］　赵彬. MIS11 阶段亚洲夏季风演化的高分辨率落水洞记录［D］. 南京：南京师范大学, 2019.

［7］　Berger A L, Loutre M F. Climate 400,000 years ago, a key to the future?［A］//Droxler A W, Poore R Z, Burckle L H. Earth's Climate and Orbital Eccentricity: The Marine Isotope Stage 11 Question. Washington, D C: American Geophysical Union,, 2003, 137: 17-26.

［8］　LIU Dianbing. Recent progress on studies of the spatial structure and dynamics for the Younger Dryas Event［J］. Geological

第 43 卷　第 2 期

XU Yibin, YANG Xunlin, YUAN Daoxian, et al: 410 ka weak monsoon event recorded by stalagmites in Jinfo Cave of Chongqing

237

Review, 2012, 58(2): 341-349.

［9］　WANG Jianli, HE Xiao, WANG Xinya, ZHANG Meiliang, LIN Yushi. Isotopic ages and paleoclimatic information from stalagmites of Chongqing Jinfushan［J］. Carsologica Sinica, 2005, 24(4): 265-269.

［10］　ZHANG Ren, ZHU Xuewen, HAN Daoshan, ZHANG Yuanhai, FANG Fengbao. Preliminary study on karst caves of Mt. Jinfo, Nanchuan,Chongqing［J］.CarsologicaSinica,1998,17(3):196-211.

［11］　Cheng H, Edwards R L, Shen C C, Polyak V J, Asmerom Y, Woodhead J, Hellstrom J, Wang Y J, Kong X G, Spötl C, Wang X F, Alexander Jr E C. Improvements in ^{230}Th dating, ^{230}Th and ^{234}U half-life values, and U-Th isotopic measurements by multi-collector inductively coupled plasma mass spectrometry［J］. Earth and Planetary Science Letters, 2013, 371-372(1): 82-91.

［12］　LI Chensi. Study on climate change of stalagmite records in Chongqing area during MIS 11［D］. Chongqing: Southwest University, 2015

［13］　Jaffey A H, Flynn K F, Glendenin L E, Bentley W C, Essling A M. Precision measurement of half-lives and specific activities of ^{235}U and ^{238}U［J］. Physical Review C, 1971, 4(5): 1889-1906.

［14］　Cheng H, Edwards R L, Sinha A, Spötl C, Yi L, Chen S T, Kelly M, kathayat G, Wang X F, Li X L, Kong X G, Wang Y J, Ning Y F, Zhang H W. The Asian monsoon over the past 640, 000 yearsandiceageterminations［J］.Nature,2016,534(7609):640-646.

［15］　Dorale J A, Liu Z H. Limitations of hendy test criteria in judging the paleoclimatic suitability of speleothems and the need for replication［J］. Journal of Cave and Karst Studies, 2009, 71(1): 73-80.

［16］　Cheng H, Sinha A, Wang X F, Cruz F W, Edwards R L. The global paleomonsoon as seen through speleothem records from Asia and the Americas［J］. Climate Dynamics, 2012, 39(5): 1045-1062.

［17］　QIN Jiaming, LIN Yushi, ZHANG Meiliang, WANG Hua, FENG Yumei, TU Linling. Change of the east-Asian monsoon climate during the last Glaciation : δ^{18}O records of stalagmites in Qixing cave, Duyun City, Guizhou Province［J］. Carsologica Sinica, 2003, 22(3): 167-173.

［18］　Liu Z Y, Wen X Y, Brady E C. Chinese cave records and the East Asia summer monsoon［J］. Quaternary Science Reviews, 2014, 83(1): 115-128.

［19］　Zhang W H, Wu J Y, Wang Y, Wang Y J, Cheng H, Kong X G, Duan F C. A detailed East Asian monsoon history surrounding the 'Mystery Interval' derived from three Chinese speleothem records［J］. Quaternary Research, 2014, 82(1): 154-163.

［20］　Porter S, Zhisheng A. Correlation between climate events in the North Atlantic and China during the last glaciation［J］. Nature, 1995, 375: 305-308.

［21］　Rohling E J, Braun K, Grant K, Kucera M, Roberts A P, Siddall M, Trommer G. Comparison between Holocene and Marine Isotope Stage-11 sea-level histories［J］. Earth and Planetary Science Letters, 2010, 291(1-4): 96-105.

［22］　Laskar J, Robutel P, Joutel F, Gastineau M, Correia A C M, Lev-rard B. A long-term numerical solution for the insolation quantities of the Earth［J］. Astronomy and Astrophysics, 2004, 428(1): 261-285.

［23］　Kandiano E S, Meer M, Schouten S, Fahl Kirsten, Sinninghe Damsté J S, Bauch H A. Response of the North Atlantic surface and intermediate ocean structure to climate warming of MIS 11［J］. Scientific Reports, 2017, 7(1): 46192.

［24］　Barker S, Chen J, Gong X, Jonkers L, Knorr G, Thornalley D. Icebergs not the trigger for North Atlantic cold events［J］. Nature Geoscience, 2015, 520: 333-336.

［25］　Kandiano E S, Bauch H A, Fahl K, Helmke J P, Röhl U, Pérez Folgado M, Cacho I. The meridional temperature gradient in the eastern North Atlantic during MI S11 and its link to the ocean–atmosphere system［J］. Palaeogeography, Palaeoclimatology, Palaeoecology, 2012, 333-334: 24-39.

［26］　Stein R, Hefter J, Grützner J, Voelker A, Naafs B D A. Variability of surface water characteristics and Heinrich-like events in the Pleistocene midlatitude North Atlantic Ocean: Biomarker and XRD records from IODP Site U1313 (MIS16–9)［J］. Paleoceanography, 2009, 24(2): 2203.

［27］　McManus J F, Oppo D W, Cullen J L, Healey S L. Marine isotope stage 11 (MIS 11): Analog for Holocene and future climate?［A］//Droxler A W, Poore R Z, Burckle L H. Earth's Climate and Orbital Eccentricity: The Marine Isotope Stage 11 Question. Washington D C: American Geophysical Union, 2003: 69-85.

［28］　Prokopenko A A, Bezrukova E V, Khursevich G K, Solotchina E P, Kuzmin M I, Tarasov P E. Climate in continental interior Asia during the longest interglacial of the past 500,000 years: The new MIS 11 records for Lake Baikal, SE Siberia［J］. Climate of the Past, 2010, 6(1): 31-48.

［29］　Oliveira D, Desprat S, Rodrigues T, Naughton F, Hodell D, Trigo R, Goni M. The complexity of millennial-scale variability in Southwestern Europe during MIS 11［J］. Quaternary Research, 2016, 86(3): 373-387.

［30］　Tzedakis P C, Pälike H, Roucoux K H, de Abreu L. Atmospheric methane, Southern European vegetation and low-mid latitude links on orbital and millennial timescales［J］. Earth and Planetary Science Letters, 2009, 277(3-4): 307-317.

［31］　Dickson A J, Beer C, Dempsey C J, Dempsey C, Maslin M A, Bendle J A, McClymont E L, Pancost R D. Oceanic forcing of the Marine Isotope Stage 11 interglacial［J］. Nature Geoscience, 2009, 2(6): 428-433.

［32］　ZHANG Taotao, LI Tingyong, HAN Liyin, CHENG Hai, LI Junyun, ZHAO Xin, ZHOU Jingli. Variation of the Asian summer monsoon during the MIS 5a/5b period inferred from a new high-resolution stalagmite record［J］. Carsologica Sinica, 2017, 36(2): 162-170.

［33］　John M D, Yuet F L, Christelle N, Dirk E, Henning A B, Adina P, Benoit T. Freshening, stratification and deep-water formation in the Nordic Seas during Marine Isotope Stage 11［J］. Quaternary Science Reviews, 2021, 272: 107231.

［34］　ZHANG Huandi, HAO Qingzhen. Marine and ice core evidence confirms delayed buildup of Arctic Ice Sheets during the MIS 11–10［J］. Quaternary Sciences, 2019, 39(3): 786-788.

［35］　Galaasen E V, Ninnemann U S, Kessler A, Irvali N, Rosenthal Y, Tjiputra J, Bouttes N, Roche D M, Kleiven H F, Hodell D A. Interglacial instability of North Atlantic deep water ventilation［J］. Science, 2020, 367(6485): 1485-1489.

［36］　Voelker A H L, Rodrigues T, Billups K, Oppo D, McManus J, Stein R, Hefter J, Grimalt J O. Variations in mid-latitude North Atlantic surface water properties during the mid-Brunhes (MIS 9–14) and their implications for the thermohaline circulation［J］. Climate of the Past, 2010, 6(4): 531-552.

［37］　Broccoli A J, Dahl K A, Stouffer R J. Response of the ITCZ to Northern Hemisphere cooling［J］. Geophysical Research Letters, 2006, 33(1): 1-4.

［38］　ZHANG Riping. The internal structure of MIS11 recorded by a stalagmite in Jinfo Cave, Chongqing and the comparison of MIS11 with Holocene［D］. Chongqing: Southwest University, 2022.

［39］　Wang X F, Auler A S, Edwards R, Cheng H, Ito E, Wang Y J, Kong X G, Solheid M. Millennial-scale precipitation changes in Southern Brazil over the past 90,000 years［J］. Geophysical Research Letters, 2007, 34(23): 135-147.

［40］　Wang Y J, Cheng H, Edwards R L, An Z S, Wu J Y, Shen C C, Dorale J A. A high-resolution absolute-dated late Pleistocene Monsoon record from Hulu cave, China［J］. Science, 2001, 294(29): 2345-2348.

［41］　Cheng H, Zhang H W, Spötl C, Baker J, Sinha A, Li H Y, Bartolomé M, Moreno A, Kathayat G, Zhao J Y, Dong X Y, Li Y W, Ning Y F, Jia X, Zong B Y, Brahim Y A, Pérez Mejiás C, Cai Y J, Novello V F, Cruz F W, Severinghaus J P, An Z S, Edwards R L. Timing and structure of the Younger Dryas event and its underlying climate dynamics［J］. Proceedings of the National Academy of Sciences, 2020, 117(38): 1-10.

［42］　EPICA community members. Eight glacial cycles from an Antarctic ice core［J］. Nature, 2004, 429: 623-628.

［43］　Stuiver M, Grootes P M. GISP2 oxygen isotope ratio［J］. Quaternary Research, 2000, 53(3): 277-284.

［44］　Haug G H, Hughen K A, Sigman D M, Peterson L C, Rohl U. Southward migration of the intertropical convergence zone through the Holocene［J］. Science, 2001, 293(5533): 1304-1308.

［45］　Hughen K A, Overpeck J T, Peterson L C, Trumbore S E. Rapid climate changes in the tropical Atlantic region during the last deglaciation［J］. Nature, 1996, 380(7): 51-54.

［46］　Hughen K A, Southon J R, Lehman S J, Overpeck J T. Synchronous radiocarbon and climate shifts during the last deglaciation［J］. Science, 2000, 290(5498): 1951-1954.

［47］　Cheng H, Li H Y, Sha L J, Sinha A, Shi Z G, Yin Q Z, Lu Z Y, Zhao D B, Cai Y J, Hu Y Y, Hao Q Z, Tian J, Kathayat G, Dong X Y, Zhao J Y, Zhang H W. Milankovitch theory and monsoon［J］. The Innovation, 2022, 3(6): 100338.

［48］　Böhm E, Lippold J, Gutjahr M, Frank M, Blaser P, Antz B, Fohlmeister J, Frank N, Andersen M B, Deininger M. Strong and deep Atlantic meridional overturning circulation during the last glacial cycle［J］. Nature, 2015, 517(7532): 73-76.

［49］　Jouzel J, Masson Delmotte V, Cattani O, Dreyfus G, Falourd S, Hoffmann G, Minster B, Nouet J, Barnola J M, Chappellaz J, Fischer H, Gallet J C, Johnsen S, Leuenberger M, Loulergue L, Luethi D, Oerter H, Parrenin F, Raisbeck G, Raynaud D, Schilt A, Schwander J, Selmo E, Souchez R, Spahni R, Stauffer B, Steffensen J P, Stenni B, Stocker T F, Tison J L, Werner M, Wolff E W. Orbital and millennial Antarctic climate variability over the past 800,000 years［J］. Science, 2007, 317(5839): 793-796.

［50］　Lisiecki L E, Raymo M E. A Pliocene–Pleistocene stack of 57 globally-distributed benthic δ^{18}O records［J］. Paleoceanography, 2005, 20(1): 1003.

［51］　Yin Q Z, Berger A. Interglacial analogues of the Holocene and its natural near future［J］. Quaternary Science Reviews, 2015, 120: 28-46.

［52］　Peter H, Carl W. Obliquity pacing of the late Pleistocene glacial terminations［J］. Nature, 2005, 434(7032): 1476-4687.

［53］　Masson Delmotte V, Dreyfus G, Braconnot P, Johnsen S, Jouzel J, Kageyama M, Landais A, Loutre M F, Nouet J, Parrenin F, Raynaud D, Stenni B, Tuenter E. Past temperature reconstructions from deep ice cores: Relevance for future climate change［J］. Climate of the Past, 2006, 2(2): 145-165.

［54］　Yin Q Z, Wu Z P, Berger A, Goosse H, Hodell D. Insolation triggered abrupt weakening of Atlantic circulation at the end of interglacials［J］. Science, 2021, 373(6558): 1035-1040.